A&A 394, 975–982 (2002)
DOI: 10.1051/0004-6361:20021227

Astronomy & Astrophysics

A high-sensitivity OH 5-cm line survey in late-type stars⋆

J.-F. Desmurs[1], A. Baudry[2], P. Sivagnanam[3], and C. Henkel[4]

[1] Observatorio Astronómico Nacional (IGN), Apartado 1143, 28800 Alcalá de Henares, Spain
[2] Observatoire de l'Université de Bordeaux, URA 352 du CNRS, BP 89, 33270 Floirac, France
[3] Observatoire de Paris, 5 place Jules Janssen, 92195 Meudon Cedex, France
[4] Max-Planck-Institut für Radioastronomie, Auf dem Hügel 69, 53121 Bonn, Germany

Received 7 May 2002 / Accepted 27 August 2002

Abstract. We have undertaken a comprehensive search for 5-cm excited OH maser emission from evolved stars representative of various stages of late stellar evolution. Observed sources were selected from known 18-cm OH sources. This survey was conducted with the 100-m Effelsberg telescope to achieve high signal to noise ratio observations and a sensitivity limit of about 0.05 to 0.1 Jy. A total of 65 stellar sources were searched for both main line and satellite line emission. We confirm the previous detection of 5 cm OH in Vy 2-2, do not confirm emission from NML-Cyg and do not report any other new detection within the above sensitivity limit.
Implications of these results on the pumping mechanism of the OH radical in circumstellar envelopes are briefly discussed.

Key words. masers – stars: AGB and post-AGB – radio lines: stars

1. Introduction

Emission from the first two rotationally excited states of OH was first discovered by Zuckerman et al. (1968) and Yen et al. (1969) for the $^2\Pi_{1/2}, J = 1/2$ and $^2\Pi_{3/2}, J = 5/2$ states, respectively. The $^2\Pi_{3/2}, J = 5/2$ state of OH lies immediately above the ground-state and gives rise to four hyperfine transitions, with the $F = 3{-}3$ and $2{-}2$ main lines at 6035.092 and 6030.747 MHz and the $F = 3{-}2$ and $2{-}3$ satellite lines at 6049.084 and 6016.746 MHz, respectively (Fig. 1). The theoretical treatment of OH excitation in star-forming regions has progressed significantly in recent years (see Cesaroni & Walmsley 1991; Gray et al. 1992; Pavlakis & Kylafis 1996), and good predictions of relative OH line intensities can be made on the basis of these models, which show the importance of multi-line studies. In the circumstellar environment of late-type stars the model developed by Elitzur et al. (1976) successfully explains the excitation of strong 1612 MHz emission. This results from a cascade of the OH population down to the $J = 1/2$ and $3/2$ states after far infrared photons at 34.6 micron and 53.3 micron (see Fig. 1) have excited the OH to the $^2\Pi_{1/2}, J = 5/2$ and $3/2$ states. There are enough far infrared photons to excite the 1612 MHz line (e.g. Epchtein et al. 1980). However, it is only recently that the direct detection of the 34.6 microns absorption line has been reported with the ISO telescope toward IRC+10420 (see Sylvester et al. 1997). Besides the conspicuous 1612 MHz line emission, 18 cm main line emission is often observed in late-type stars. Conditions for this emission are carefully investigated in the work of Collison & Nedoluha (1994, 1995) and we discuss later in this work the implication of their excitation mechanism for the $J = 5/2$ state of OH.

The main goal of the present observations was to survey the 5 cm Λ doublet lines of OH in a number of stars ranging from typical Miras to OH/IR objects or pre-planetary nebulae. These stars sample various late stages of stellar evolution. In addition, observations of the $^2\Pi_{3/2}, J = 5/2$ state lying immediately above the ground-state provide a critical test for OH excitation models.

These observations and our results obtained in 65 sources are presented in Sects. 2 and 3. Some OH properties of selected stars are also presented in Sect. 3. In Sect. 4 we discuss stellar OH pumping schemes and variability of OH main line emission sources in the light of our results.

2. Observations

Observations were made with the 100-m antenna at Effelsberg[1] in December 1999. We used a cooled HEMT dual-channel receiver connected to only one sense of polarization, Left Circular Polarization (LCP). The system temperature was ≈60 K ($T_{\rm mb}$) including ground pick up and sky noise. We

Send offprint requests to: J.-F. Desmurs, e-mail: desmurs@oan.es

⋆ Table 1 is also available in electronic form at the CDS via anonymous ftp to cdsarc.u-strasbg.fr (130.79.128.5) or via http://cdsweb.u-strasbg.fr/cgi-bin/qcat?J/A+A/394/975

[1] The 100-m telescope at Effelsberg is operated by the Max-Planck-Institut für Radioastronomie (MPIfR) on behalf of the Max-Planck-Gesellschaft (MPG).

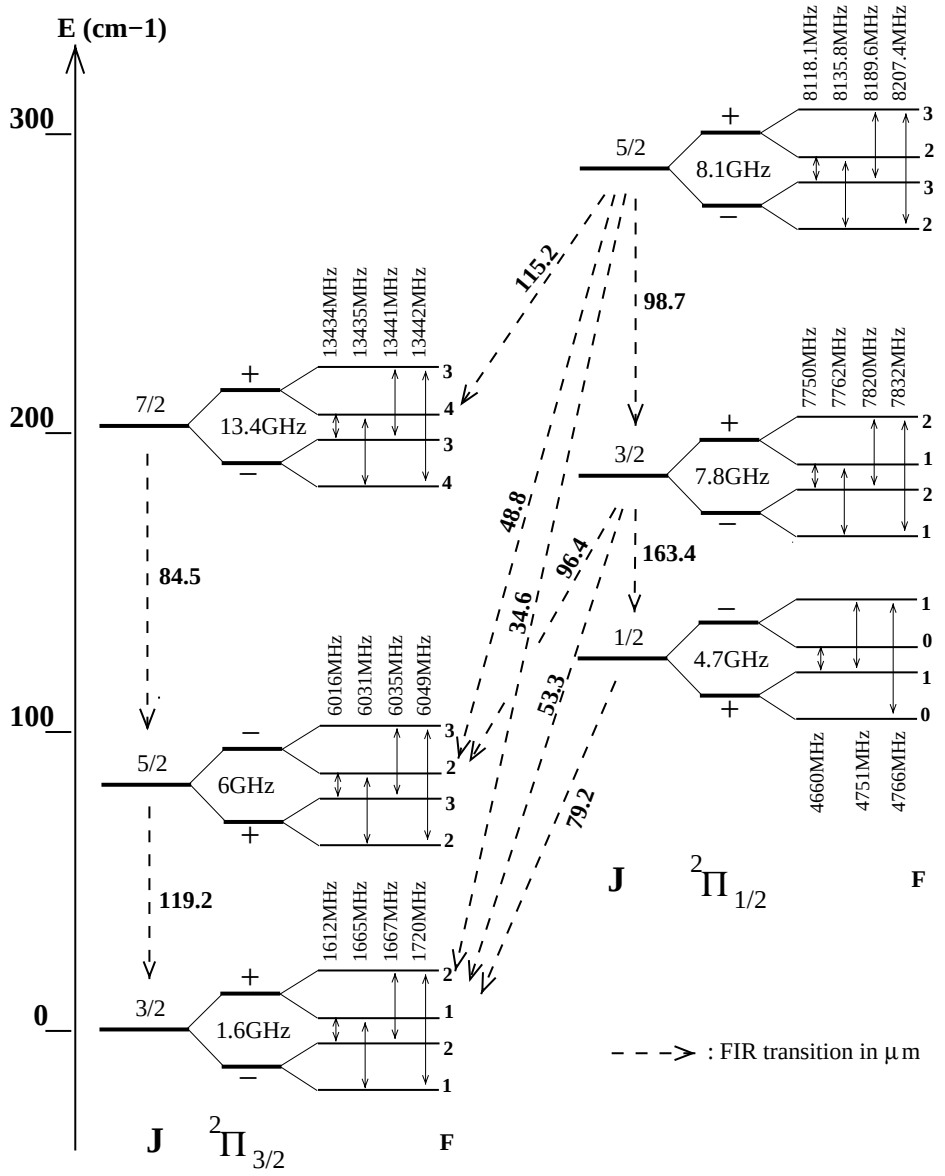

Fig. 1. The energy level diagram for the $^2\Pi_{3/2}$ and $^2\Pi_{1/2}$ ladders of OH. Λ doubling (not to scale) and parities are shown in each case. Transitions between the $F = 3$ and 2 hyperfine levels, for $^2\Pi_{3/2}$, $J = 5/2$, give rise to the four 6 GHz lines.

used a position switching observing mode with the reference position offset by 600″ in longitude from the source position (the half-power beamwidth of the telescope at 6 GHz is 130″). The new auto-correlator AK90 was split into 2 bands of 20 MHz each thus allowing us to simultaneously observe the 2 main lines and the two satellites lines of the $J = 5/2$ state. There were 4096 channels per band giving a channel separation of 4.9 kHz and thus an effective spectral velocity resolution of 0.29 km s^{-1}. Proper functioning of the system was checked by observations of the strong 5 cm OH emission from the two compact HII regions W3(OH) and ON1 (see Table 1).

Calibration of the data followed the procedure used in the 6 GHz survey of star-forming regions made by Baudry et al. (1997). OH spectra were calibrated in terms of the noise source coupled to one polarization channel and the flux density scale was determined by observations of NGC 7027 (Ott et al. 1994). The noise tube was calibrated in Jy assuming that the 6 GHz flux density of NGC 7027 was 5.9 Jy. We estimate that the flux density scale uncertainty is within 10%. All spectra were calibrated in terms of single polarization flux densities. This is one-half of the two polarization flux density. For possible 5 cm radio interference, we proceeded as in Baudry et al. (1997).

Our input catalog is listed in Table 1. It is based on 18 cm OH data. We selected sources which clearly exhibit the 1612 MHz satellite line and/or the 1665/1667 main lines. By these means we obtained targets with noticeable amounts of OH molecules and IR photons, that are not excessively distant in order to be detected.

The sources are essentially OH Miras with thin or moderately thick envelopes, and thick OH/IR objects. Bright Miras with both satellite and main lines were selected, from the Sivagnanam et al. (1988) comprehensive OH survey of the 1-kpc solar neighborhood. Most of them are also known as 22 GHz water maser sources. From the David et al. (1993)

Table 1. Observations of the 6GHz OH maser transitions in AGB stars.

IRAS Source	Other Name	Type[1]	Observed Coordinates J2000.0[3]		Observed Velocity Range, LSR	Sensitivity[2] (Jy) (at 3σ) 6 GHz LCP
			RA h m s	Dec ° ′ ″	(km s^{-1})	
02232+6138	W3(OH)	UCHII	2:27:03.866	+61:52:24.82	−939/+998, (−45.0)	E
20081+3122	ON1	UCHII	20:10:09.073	+31:31:34.40	−894/1043, (+00.0)	E
00007 + 5524	Y Cas	Mira main	00:03:21.605	+55:40:48.21	−911/1026, (−17.0)	0.08
01037 + 1219	IRC+10011	OH/IR Moderate	01:06:25.965	+12:35:53.07	−886/1051, (+08.0)	0.07
02168 − 0312	OMI Cet	Mira main	02:19:20.679	−02:58:39.21	−848/1089, (+46.0)	0.06
02192 + 5821	S Per	SG	02:22:51.689	+58:35:11.76	−932/1005, (−38.0)	0.08
02251 + 5102	RR Per	Mira main	02:28:29.318	+51:16:17.60	−894/1043, (+00.0)	0.08
02420 + 1206	RU Ari	Mira sat	02:44:45.184	+12:19:08.15	−874/1063, (+20.0)	0.07
03206 + 6521	OH 138.0+7.2	OH/IR Moderate	03:25:08.552	+65:32:05.42	−931/1006, (−37.5)	0.08
03293 + 6010	OH 141.0+3.5	OH/IR Moderate	03:33:30.528	+60:20:09.10	−951/986, (−57.2)	0.07
03507 + 1115	IK Tau	Mira sat	03:53:28.983	+11:24:20.02	−861/1076, (+33.0)	0.05
05073 + 5248	NV Aur	OH/IR Moderate	05:11:19.747	+52:52:27.79	−891/1046, (+02.9)	0.08
05131 + 4530	RAFGL 712	OH/IR Moderate	05:16:47.103	+45:34:03.76	−926/1011, (−32.3)	0.09
05528 + 2010	U Ori	Mira sat	05:55:49.264	+20:10:30.77	−933/1004, (−39.5)	0.04
05559 + 7430	V Cam	Mira main	06:02:32.779	+74:30:27.26	−887/1050, (+06.5)	0.07
06297 + 4045	OH 174.7+13.5	OH/IR Moderate	06:33:14.921	+40:42:49.71	−910/1027, (−16.3)	0.08
06363 + 5954	U Lyn	Mira main	06:40:46.320	+59:52:00.23	−904/1033, (−10.0)	0.07
06500 + 0829	GX Mon	Mira sat	06:52:42.408	+08:25:23.33	−905/1032, (−11.0)	0.06
07209 − 2540	VY Cma	SG	07:22:58.17	−25:46:02.95	−872/1065, (+22.0)	0.07
07399 − 1435	OH231.8+4.2	PPN	07:42:16.738	−14:42:14.04	−878/1059, (+16.0)	0.06
07422 + 3054	AU Gem	Mira Main	07:45:27.590	+30:46:43.11	−890/1047, (+04.0)	0.04
07585 − 1242	U Pup	Mira sat	08:00:50.596	−12:50:31.88	−912/1025, (−18.0)	0.04
08005 + 2356		OH/IR Late	08:02:59.186	+23:45:33.23	−888/1049, (+05.7)	0.07
08357 − 1013	OH235.3+18.1	OH/IR Moderate	08:38:08.805	−10:24:16.95	−894/1043, (+00.0)	0.07
09425 + 3444	R Lmi	Mira main	09:45:34.314	+34:30:42.91	−894/1043, (+00.0)	0.14
09448 + 1139	R Leo	Mira main	09:47:33.446	+11:25:43.52	−893/1044, (+01.0)	0.05
10580 − 1803	R Crt	SR	11:00:33.822	−18:19:29.54	−884/1053, (+10.0)	0.05
12562 + 2324	T Com	Mira sat	12:58:38.600	+23:08:23.03	−879/1058, (+15.0)	0.07
13001 + 0527	RT Vir	SR	13:02:37.908	+05:11:08.56	−876/1061, (+18.0)	0.09
14247 + 0454	RS Vir	Mira sat	14:27:16.393	+04:40:40.38	−894/1043, (+00.0)	0.08
15193 + 3132	S Crb	Mira main	15:21:24.366	+31:22:02.05	−894/1043, (+00.0)	0.07
15255 + 1944	WX Ser	Mira sat	15:27:47.009	+19:34:02.33	−888/1049, (+06.0)	0.08
16235 + 1900	U Her	Mira main	16:25:47.411	+18:53:32.98	−907/1030, (−13.0)	0.05
18006 − 1734	GLMP 704	OH/IR Late	18:03:36.581	−17:34:00.59	−870/1067, (+23.9)	0.10
18071 − 1727	OH 12.8 +.9	OH/IR Late	18:10:05.813	−17:26:35.22	−868/1069, (+25.9)	0.09
18081 − 0338		OH/IR Thick	18:10:49.074	−03:38:14.46	−889/1049, (+05.6)	0.08
18100 − 1915	GLMP 740	OH/IR Thick	18:13:02.725	−19:14:20.42	−876/1061, (+17.6)	0.09
18107 − 0710		OH/IR Thick	18:13:29.720	−07:09:48.92	−876/1061, (+17.9)	0.08
18135 − 1456	OH 15.7 +.8	OH/IR Late	18:16:26.004	−14:55:13.43	−895/1042, (−01.1)	0.09

Nançay survey of OH/IR objects, we retained bright 1612 MHz sources with detected 1667 MHz emission. Targets have been chosen in order to sample objects lying along the sequence drawn by evolved stars in the IRAS two-color diagram (see Fig. 2). They mostly belong to the AGB. This sequence of envelope thicknesses is thought to reflect various evolutionary stages, and a certain initial mass distribution. Given our selection criteria we favored the best candidate stars for showing OH maser emission i.e. the nearby OH/IR stars with high luminosity and large amounts of dust and infrared photons.

We also included in our survey a few typical Semi-Regular variables, Proto-Planetary Nebulae (PPN), and Planetary Nebulae (PN), that are thought to be linked to the same evolutionary tracks. We added some red Supergiants (SG).

Table 1. continued.

IRAS Source	Other Name	Type[1]	Observed Coordinates J2000.0[3]		Observed Velocity Range, LSR	Sensitivity[2] (Jy) (at 3σ)
			RA	Dec		6 GHz
			h m s	° ′ ″	(km s^{-1})	LCP
18152−0919	OH 20.8 +3.1	OH/IR Thick	18:17:58.662	−09:18:42.44	−867/1070, (+26.7)	0.08
18198−1249	OH 18.3 +.4	OH/IR Late	18:22:43.046	−12:47:40.94	−846/1091, (+48.0)	0.10
18262−0735		OH/IR Thick	18:28:59.446	−07:33:25.44	−815/1122, (+78.9)	0.08
18268−1117	OH 20.4 -.3	OH/IR Thick	18:29:35.755	−11:15:53.97	−852/1085, (+41.8)	0.08
18266−1239	V435 Sct	OH/IR Thick	18:29:28.605	−12:37:40.55	−844/1093, (+50.0)	0.08
18348−0526	V437 Sct	OH/IR Thick	18:37:31.986	−05:23:59.35	−867/1070, (+27.2)	0.06
18432−0149	V1360 Aql	OH/IR Thick	18:45:52.691	−01:46:43.27	−828/1109, (+66.2)	0.08
18460−0254	V1362 Aql	OH/IR Late	18:48:40.999	−02:50:22.29	−795/1142, (+99.0)	0.09
18488−0107	V1363 Aql	OH/IR Late	18:51:25.772	−01:03:54.48	−818/1119, (+75.8)	0.08
18525+0210		OH/IR Thick	18:55:04.815	+02:14:41.21	−823/1113, (+70.2)	0.07
18549+0208	OH 35.6 -.3	OH/IR Thick	18:57:26.573	+02:12:11.24	−816/1121, (+77.9)	0.09
18560+0638	V1366 Aql	OH/IR Moderate	18:58:30.142	+06:42:55.91	−874/1063, (+19.7)	0.10
19039+0809	R Aql	Mira sat	19:06:22.196	+08:13:48.16	−846/1091, (+48.0)	0.09
19065+0832	OH 42.6 +.0	OH/IR Late	19:08:58.368	+08:37:47.08	−841/1096, (+53.1)	0.07
19071+0946	OH 43.8 +.5	OH/IR Thick	19:09:31.065	+09:51:54.41	−885/1052, (+09.1)	0.12
19161+2343		OH/IR Moderate	19:18:14.537	+23:49:26.23	−865/1072, (+28.6)	0.07
19219+0947	Vy 2-2	PN	19:24:22.078	+09:53:55.82	−956/981, (−44.3)	E/0.02
19244+1115	V1302 Aql	OH/IR Moderate	19:26:47.588	+11:21:14.77	−849/1088, (+45.0)	0.08
19343+2926	M1-92	PPN	19:36:16.768	+29:32:15.80	−894/1043, (+0.00)	0.24
19352+2030		OH/IR Thick	19:37:23.395	+20:39:21.86	−889/1048, (+05.0)	0.20
20043+2653	GLMP 972	OH/IR Thick	20:06:22.890	+27:02:11.23	−898/1039, (−04.6)	0.08
20047+1248	SY Aql	Mira sat	20:07:05.694	+12:57:07.39	−943/994, (−49.0)	0.08
NML Cyg		SG	20:46:25.941	+40:06:56.09	−894/1043, (+00.0)	0.02
20491+4236	OH 83.4 -.9	OH/IR Moderate	20:50:57.766	+42:48:04.31	−932/1005, (−38.4)	0.05
21554+6204	GLMP 1048	OH/IR Thick	21:56:58.184	+62:18:43.62	−914/1022, (−20.6)	0.06
22177+5936	NSV 25875	OH/IR Moderate	22:19:27.806	+59:51:21.74	−919/1017, (−25.6)	0.07
23041+1016	R Peg	Mira main	23:06:38.829	+10:32:37.94	−870/1067, (+24.0)	0.09
23558+5106	R Cas	Mira main	23:58:24.683	+51:23:18.18	−870/1067, (+24.0)	0.06

[1] UCHII: Ultra Compact HII region, SG: Supergiante, SR: Semi Regular, PN: Planetary Nebulae, PPN: Proto Planetary Nebulae.
[2] E = Emission; the upper limits correspond to 3σ.
[3] B1950 coordinates processed to J2000 within GILDAS package.

The latter are luminous massive stars that are not on the AGB, but which usually present somewhat similar circumstellar envelopes. In our input catalog are NML Cyg (SG) and Vy 2–2 (PN), for which tentative detections at 5 cm have been reported in the literature.

3. Results

3.1. Previous surveys

Previous attempts made to search for excited OH from circumstellar envelopes gave only negative or controversial results with the exception of one object. As far as we are aware only a few searches for $J = 1/2$ and 5/2 OH emission at 4.7 and 6 GHz from stars have been undertaken (see Thacker et al. 1970; Zuckerman et al. 1972; Baudry 1974; Claussen & Fix 1981; Jewell et al. 1985). The latter work was the most sensitive search for excited OH from stars yet performed. Zuckerman et al. (1972) reported weak 6035 MHz ($^2\Pi_{3/2}, J = 5/2$) emission from NML Cyg and Claussen & Fix (1981) reported weak 4751 MHz ($^2\Pi_{1/2}, J = 1/2$) emission from AU Gem. However, both detections were not confirmed by Jewell et al. (1985). On the other hand, Jewell et al., reported weak 6035 MHz maser emission from the planetary nebula Vy 2–2 appearing at the same velocity, −62 km s^{-1}, as the peak 1612 MHz maser emission detected by Davis et al. (1979).

3.2. New Effelsberg survey

In Table 1, we list the 65 late type stars observed by us. For all sources, the velocity range of search for emission is given

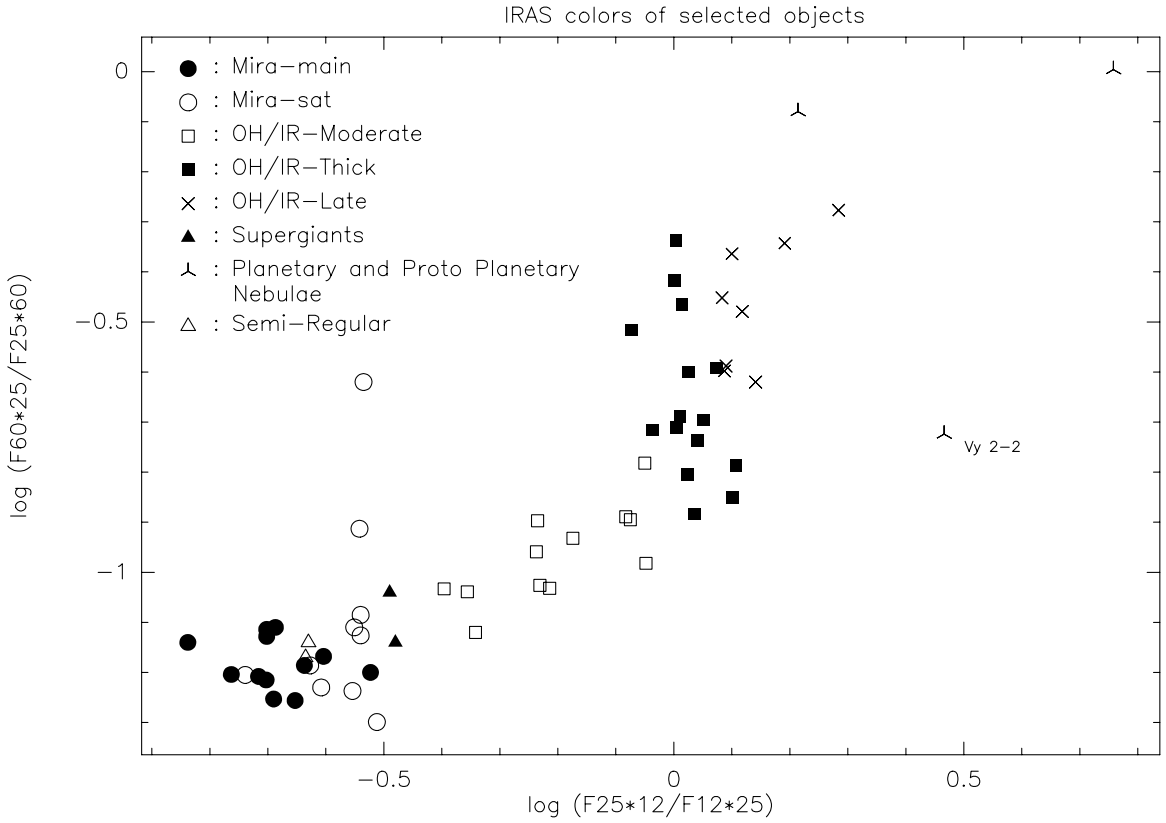

Fig. 2. Uncorrected IRAS colors from IRAS flux measurements available of the sources in our sample. (NML Cyg is not included as there is no IRAS measurement available.)

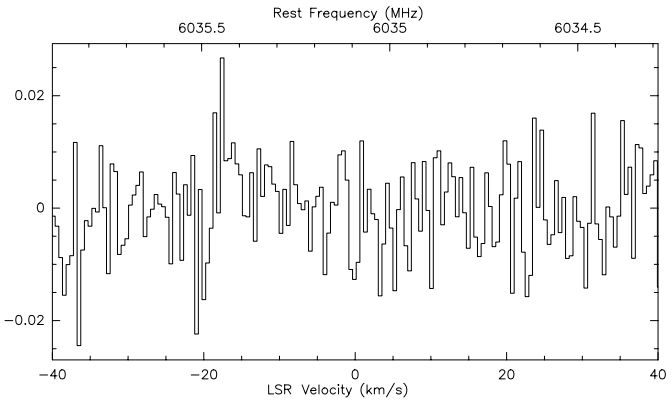

Fig. 3. The 6 GHz spectra obtained in Dec 1999 for NML Cyg, the rms at 1σ is ~6mJy (LCP spectrum). No detection reported.

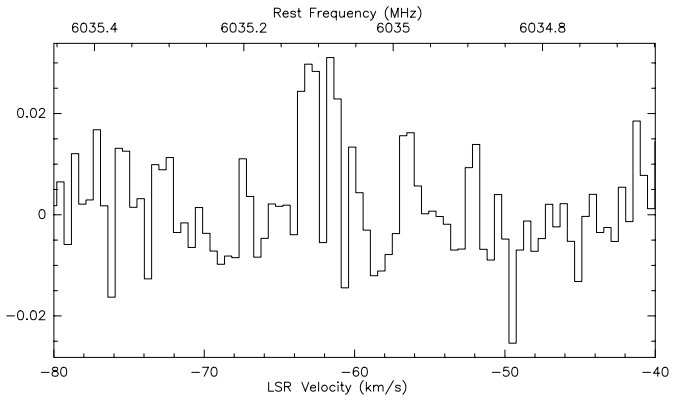

Fig. 4. 6035 MHz OH spectrum obtained in Dec. 1999 from Vy 2–2. The line intensity is in Jy for single polarization, the rms at 1σ is ~6mJy.

(with the systemic velocity in parenthesis), together with the sensitivity limit achieved in our new survey at 3σ. The average noise level reached in our survey is (at 3σ with a channel width of 0.29 km s^{-1}) around 80 mJy; in comparison, Jewell et al. (1985) have reached about 230 mJy (with a channel width of 0.06 km s^{-1}).

Of the 65 sources observed, no one exhibits a clear emission or absorption signal. There are however two sources with tentative detections, NML Cyg (see Fig. 3) and Vy 2–2 (Fig. 4). For NML Cyg, we reached the sensitivity of 20 mJy (at 3σ level) over the observing LSR velocity range. The 0.8 K (2.2Jy) signal reported by Zuckerman et al. (1972) and lying close to +5 km s^{-1}, would have been easily detected by us. However, we can not exclude that the emission varies with time. The tentative feature at about −17 km s^{-1} (Fig. 4) is only detected at a $\sim 3\sigma$ level and is therefore not convincing, but we note that 1612 MHz line emission at −18 km s^{-1} has been reported previously (see e.g. Engels 1979).

The case of Vy 2–2 is different. With an integrated intensity of ~48 mJy km s^{-1}, we have obtained a 6σ detection. Only the F = 3–3 maser line transition lying at 6035 MHz was detected. No absorption or emission can be observed for the other transitions. Figure 4 shows the observed 6035 MHz spectrum.

Table 2. Gaussian line parameters of the 6035 MHz OH emission line of Vy 2–2.

Velocity (km s^{-1})	Peak flux density (mJy)	Linewidth (km s^{-1})
−63.0 ± 0.14	38 ± 8	1.14 ± 0.17
−61.6 ± 0.14	39 ± 8	0.84 ± 0.17

The parameters and uncertainties (1σ) of Gaussian fits to the detected features are displayed in Table 2. The derived apparent luminosity is 1.1 Jy km s^{-1}kpc^2 (assuming a distance of 3.8 kpc, Bensby & Lundström 2001). The lack of $F = 2$–2 emission[2] and the narrow $F = 3$–3 linewidth suggest that the observed $F = 3$–3 line results from a maser process. However, only interferometric observation could give a definitive proof of it.

This detection is consistent with the results of Jewell et al. (1985) who observed maser emission at nearly the same velocity (∼−62.3 km s^{-1}) and with about the same line width (∼1.5 km s^{-1}) but with a peak flux intensity four times stronger (0.15 Jy). The presence of the two features (Fig. 4) is likely real. After splitting our data in two equal parts, the same two components appear. In another data reduction test, we have degraded our spectral resolution. This yields one single feature with a line width of ∼2.5 km s^{-1}, i.e. twice the line width observed by Jewell et al., centered around −62.3 km s^{-1}. Our observations and data reduction confirm long term OH emission from Vy 2–2.

3.3. Vy 2–2

As is the case for other Galactic planetary nebulae, the distance to Vy 2–2 (G045.4-02.7) is poorly known. Previous attempts to determine the distance have resulted in a wide range of estimates. Those estimates put this object from 1.9 kpc (see Acker 1978) based on an optical calibration to a kinematic distance of 20 kpc (Davis et al. 1979). The most recent estimate, based on a compilation of previous measurements (see Bensby & Lundström 2001) gives a distance of 3.8 kpc. Vy 2–2 is a source of free-free radio continuum radiation and dust-type infrared emission. VLA maps show a slightly elongated continuum source (Seaquist & Davis 1983). The continuum emission originates from a compact (diameter ∼ 0.5″) and narrow (thickness ∼< 0.″12) shell of ionized gas. This ionized region is surrounded by an extended halo of over 25″ in radius, detected through its Hα line emission (see Miranda & Solf 1991). From the visibility analysis, Christianto & Seaquist (1998) estimate an angular expansion of 1.13 ± 0.12 mas/yr^{-1}. This would give for a distance of 3.8 kpc an expansion velocity of about 20 km s^{-1}, in contradiction with the expansion velocity of 6 km s^{-1} measured by Miranda & Solf (1991) in the equatorial plane and qualified to be slow. Taking a systemic velocity for the source of −44.3 ± 1.0 km s^{-1} (tentative detection of Knapp & Morris 1985) this would give a blue-shifted velocity for the OH maser of about 20 km s^{-1}. The inferred expansion velocity is then in good agreement with the value derived by Christianto & Seaquist (1998) for a distance of 3.8 kpc. The kinematic age of the nebula they derived is 213 years and supports the conclusion that this object is a very young planetary nebula. The temperature of the central star is estimated to be greater than 35 000 K (see Zijlstra et al. 1989; Clegg & Walsh 1989). The dust color temperature was estimated by Cohen & Barlow (1974) to be less than 190K.

Jewell et al. (1985) and Cohen et al. (1991) searched without success for $^2\Pi_{1/2}, J = 1/2$ maser emission (down to a 3σ limit of ∼0.25 Jy). The 1612 MHz maser emission, the only ground-state maser transition observed, was first detected by Davis et al. (1979). Seaquist & Davis (1983) located the maser at the front edge of the ionized shell, coincident with a shock front and an ionization front, placing the OH maser on the near side of the expanding shell and thus providing an explanation for the blue-shifted maser feature. This is consistent with the fact that OH molecules are effectively produced in the outer parts of circumstellar envelopes due to photoionization of H_2O by interstellar UV photons. The typical abundance for OH molecules relative to H_2 is about 10^{-5} and HST observations (see Sahai & Trauger 1998) show a compact bright bipolar source expanding along an axis roughly orthogonal to the bipolar axis. Despite the fact that almost all planetary nebulae appear optically thin at 5 GHz, Vy 2–2 is optically thick (see Purton et al. 1982).

4. Implications on pumping schemes

There exist two main ways to invert the 5 cm maser transition, (1) by radiative pumping of far infrared (FIR) photons or (2) by collisions with H_2 molecules (in combination with local and non-local line overlap). Chemical pumping does not seem applicable and interstellar UV photons are only responsible for the dissociation of H_2O molecules in the outer part of the circumstellar envelope to produce OH (the contribution of stellar UV photons is negligible except perhaps for the inner regions of the envelope).

4.1. About the ground-state masers

Theoretical studies of the pumping mechanism of the 18 cm OH lines are quite advanced. The absorption of FIR photons at 34.6 μm and 53.3 μm excites the OH from the ground state to the $^2\Pi_{1/2}$ ladder. Subsequent cascading of the populations through the $J = 1/2$ and $J = 3/2$ levels inverts the $J = 3/2$ ground state (Elitzur et al. 1976). This scheme explains rather well the strong 1612 MHz line and essentially avoids the $^2\Pi_{3/2}$ ladder (Davis et al. 1979). Therefore, in circumstellar regions where 1612 MHz is strong and the above mechanism prevails one should not expect to detect 5 cm OH emission.

However, the pump cycle may differ in inner layers where highly excited lines are expected to be found. Moreover, Collison & Nedoluha (1994, 1995) argue that FIR line overlaps are also important to enhance the 1612 MHz line and may even be the primary inverting scheme for the 1612 MHz line in not too optically thick OH envelopes. In the latter case

[2] In the LTE approximation we obtain $F = 3$–$3/F = 2$–2 approx 1.4 whereas we observe here >2.

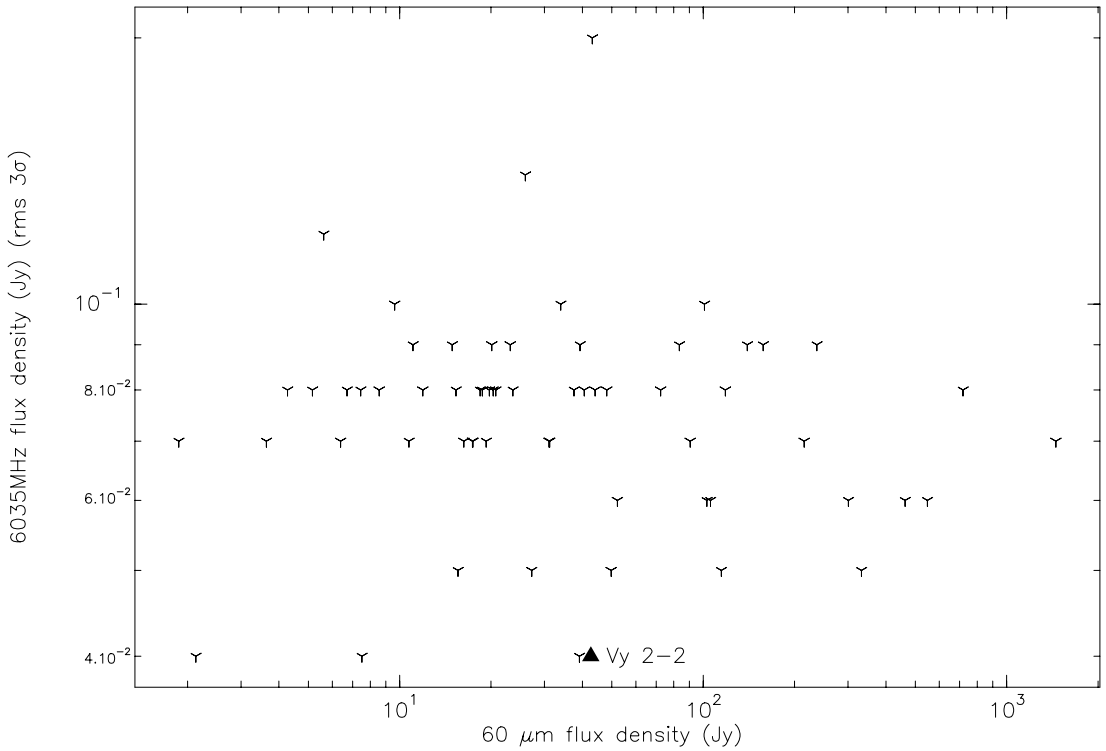

Fig. 5. IRAS 60 μm versus the OH 6035 MHz 3σ flux density limit (channel 0.25 km s^{-1}). The filled triangle corresponds to the only detection in our sample, Vy 2–2, the detected flux is given.

overlaps at 120 μm are important and populating the J = 5/2 level is essential. Collison & Nedoluha (1994) argue that FIR line overlaps alone cannot explain the main-line masers in stars (contrary to earlier models) and that near infrared (NIR) overlap effects (with OH or H_2O) are likely needed to explain the main line emission from thin circumstellar shells.

The most recent model published on OH masers in circumstellar envelopes (see Thai-Q-Tung et al. 1998) treats only the ground-state excitation and considers two models. The first one is with line overlapping limited by a Doppler shift of 2 km s^{-1} and the other one with large overlapping (up to the expansion velocity). In both models the 1612 MHz appears much stronger than the other ground state lines by a factor 10^2 to 10^3. They found that the pumping based on FIR hyperfine line overlapping is much smaller in the second case. They suggest that FIR line overlapping occurs inside clumps (small Doppler shift) of circumstellar envelopes (this idea was also invoked by Collison and Nedoluha), but no prediction is made about the excited state. Only the recent work of Pavlakis & Kylafis (1996, 2000) studied excited OH maser emission but only in the case of massive star forming regions.

Modeling the detected maser emission in Vy 2–2 at 1612 and 6035 MHz is a challenge. The particular nature of the source, a very young proto planetary nebulae, may certainly be a clue. The fact that two masers are observed at the same LSR velocity (−62 km s^{-1}) argues in favor of their spatial association. In such a case they would both originate from the thin ionization shell presenting similar conditions as in HII regions. Within this context, PPN shells may be characterized by particularly high densities and long path lengths for coherent amplification that have to be taken into account.

4.2. Infrared pumping?

Excitation of the OH radical results from complex competitive schemes involving both collisional and radiative pumping as well as line overlap effects that are correlated with the velocity field in the OH medium and local line broadening. The 5 cm OH lines arise from energy levels 84 cm^{-1} above the ground-state and we therefore expect that FIR photons around 100 μm are involved in the OH pumping cycle. To evaluate the possibility of a pumping scheme based only on IR photons, Fig. 5 compares the IRAS flux at 60 μm and the lower limits of OH emission at 6 GHz, assuming that the ratio between the radio solid angle and the IR solid angle is ≈1. Figure 5 shows that the number of FIR photons largely exceeds the emitted radio photons. Baudry et al. (1997) reached a similar conclusion for compact HII regions but in that case many 5 cm OH masers could be detected. From this we conclude that in stellar envelopes the OH pumping mechanism is different from that in massive star forming regions and that the available FIR radiation is unlikely to work as a pump for this maser. Moreover as the envelopes are dense, it is possible that even if the IR pumping were efficient, collisions could effectively quench the OH maser emission.

5. Conclusion

We have observed an extensive sample of OH/IR stars and late-type variables. Except for one atypical source (Vy 2–2) no excited OH maser has been detected. We do not confirm

the tentative detection of NML Cyg. Only the blue shifted emission is detected in Vy 2–2 for which we have discussed briefly the morphology and OH production. The absence of detectable excited emission at 5 cm (except the unique object Vy 2–2) tends to argue in favor of a pumping scheme based essentially on the absorption of 35 and 53 μm photons. In the case of Vy 2–2 the ionization shell from where the maser emission seems to originate, may present physical conditions (shock, higher temperature and density) similar to those prevailing in HII regions. A hybrid pumping model applying to both OH/IR stars and HII regions or even a pumping scheme similar to OH maser emission in massive star forming regions may be successful. It is interesting to note that no absorption at 35 and 53 μm can be seen for this source in ISO observations. Interferometric observations are needed to spatially determine the likely related positions of the 1612 and 6035 MHz maser emission in Vy 2–2.

Acknowledgements. This research has made use of the SIMBAD database operated at CDS, Strasbourg, France and ASTRID database, operated at GRAAL, Montpellier, France. We thank Dr A. M. S. Richard for valuable suggestions to prepare the observations and N. J. Rodríguez-Fernández for his help on ISO data.

References

Acker, A. 1978, A&AS, 33, 367
Baudry, A. 1974, A&A, 32, 191
Baudry, A., Desmurs, J.-F., Wilson, T. L., & Cohen, R. J. 1997, A&A, 325, 255
Bensby, T., & Lundström, I. 2001, A&A, 374, 599
Cesaroni, R., & Walmsley, M. C. 1991, A&A, 241, 537
Christianto, H., & Seaquist, E. R. 1998, AJ, 115, 2466
Claussen, M. J., & Fix, J. D. 1981, ApJ, 250, L77
Clegg, R., & Walsh, J. R. 1989, IAU, 131, p443
Cohen, M., & Barlow, M. J. 1974, ApJ, 193, 401
Cohen, M., Masheder, M. R. W., & Walker, R. N. F. 1991, MNRAS, 250, 611
Collison, A. J., & Nedoluha, G. E. 1994, ApJ, 422, 193
Collison, A. J., & Nedoluha, G. E. 1995, ApJ, 442, 311
David, P., Le Squeren, A. M., & Sivagnanam, P. 1993, A&A, 277, 453
Davis, L. E., Seaquist, E. R., & Purton, C. R. 1979, ApJ, 230, 434
Elitzur, M., Goldreich, P., & Scoville, N. 1976, ApJ, 205, 384
Engels, D. 1979, A&AS, 36, 337
Epchtein, N., Guibert, J., Nguyen-Quang-Rieu, Mr., Turon, P., & Wamsteker, W. 1980, A&A, 85, L1
Gray, M. D., Field, D., & Doel, R. C. 1992, A&A, 262, 555
Jewell, P. R., Schenewerk, M. S., & Snyder, L. E. 1985, ApJ, 295, 183
Knapp, G. R., & Morris, M. 1985, ApJ, 292, 640
Miranda, L. F., & Solf, J. 1991, A&A, 252, 331
Moore, T. J. T., Cohen, R. J., & Mountain, C. M. 1988, MNRAS, 231, 887
Ott, M., Witzel, A., Quirrenbach, A., et al. 1994, A&A, 284, 331
Pavlakis, K. G., & Kylafis, N. D. 1996, ApJ, 467, 300
Pavlakis, K. G., & Kylafis, N. D. 1996, ApJ, 467, 309
Pavlakis, K. G., & Kylafis, N. D. 2000, ApJ, 534, 770
Purton, C. R., Feldman, P. A., Marsh, K. A., Allen, D. A., & Wright, A. E. 1982, MNRAS, 198, 321
Sahai, R., & Trauger, J. T. 1998, AJ, 116, 1357
Seaquist, E. R., & Davis, L. E. 1983, ApJ, 274, 659
Sivagnanam, P., Le Squeren, A. M., & Foy, F. 1988, A&A, 206, 285
Sylvester, R. J., Barlow, M. J., Liu, X. W., et al. 1997, MNRAS, 291, L42
Thacker, D. L., Wilson, W. J., & Barrett, A. H. 1970, ApJ, 161, L191
Thai-Q-Tung, Dinh-V-Trung, Nguyen-Q-Rieu, et al. 1998, A&A, 331, 317
Yen, J. L., Zuckerman, B., Palmer, P., & Penfield, H. 1969, ApJ, 156, L27
Zijlstra, A. A., Te Lintel Hekkert, P., Pottasch, S. R., et al. 1989, A&A, 217, 157
Zuckerman, B., Palmer, P., Penfield, H., & Lilley, A. E. 1968, ApJ, 153, L69
Zuckerman, B., Yen, J. L., Gottlieb, C. A., & Palmer, P. 1972, ApJ, 177, 59